HERON is jointly edited by:
STEVIN-LABORATORY of the department of Civil Engineering, Delft University of Technology, Delft, The Netherlands
and
INSTITUTE TNO for Building Materials and Building Structures. Rijswijk (ZH), The Netherlands.
HERON contains contributions based mainly on research work performed in these laboratories on strength of materials, structures and materials science.

Secretary:
G. J. van Alphen
Stevinweg 1
P.O. Box 5048
2600 GA Delft, The Netherlands
Tel. 0031-15-785919
Telex 38070 BITHD

HERON vol. 28 1983 no. 2

Contents

DEVELOPMENT OF STADIF, A SPECIAL VERSION OF THE PROGRAM, ON THE BASIS OF FINITE DIFFERENCES

A. K. de Groot

Publications in HERON since 1970

PROGRESS IN RESEARCH ON REINFORCED CONCRETE PLANE FRAMES

Preface

The analysis of the non-linear behaviour of reinforced concrete framed structures has long been the subject of investigation in various countries, including the Netherlands. Over the years, articles on the subject by A. K. de Groot and A. C. van Riel (1967, Nos. 3/4), Th. Monnier (1970, No. 1) and J. Blaauwendraad (1972, No. 4) have been published in this journal.

De Groot and Van Riel studied the behaviour of plain (unreinforced) columns and used finite-difference analysis in their investigations. Monnier analysed the behaviour of continuous beams using experimentally determined moment-curvature diagrams. Blaauwendraad, finally, proposed a general method for plane frames, adopting an approach which tied up with the finite element method. He determined the non-linear stiffness matrix of a bar-type member on the basis of an assumed displacement field and of the constitutive properties of the materials concrete and steel. The computer program designated as STANIL, which was developed in the context of those investigations, is still used in the Netherlands, more particularly in research projects.

After the publication which appeared in 1972, this program, i.e., STANIL, underwent continuous further development. In 1974 C. Gouwens, in his graduation assignment in the Department of Civil Engineering of the Delft University of Technology, cast the program in a different mould. He rewrote it in such a way that the loading could be increased incrementally in order thus to keep closer track of any particular loading procedure. The option of tensioning stiffening was also included in the program. Later on, a special version of this program was produced within the context of the Concrete Mechanics project of CUR-VB Committee A26 and was the subject of an article published in Heron, 1981, No. 1c. Called STANIL/1, that special version is characterized by, among other features, the fact that shear deformation is taken into account, so that the forces developed in stirrups or binders can also be calculated.

The two subjects dealt with in this latest issue of Heron are again concerned with the STANIL program. The first subject relates to an application thereof, and the second to a new modified version called STADIF.

The application has reference to research which is being performed, in the Netherlands, on beam-to-column connections by CUR-VB Committee C28 "Structural details".

Experimental research has shown that such connections may possess less strength and rigidity than is normally assumed in structural calculations. By making use of the STANIL program it becomes possible to obtain insight into the residual strength of a framed structure as a whole in the case of possible imperfections of its beam-to-column connections. The authors, J. Blaauwendraad and A. K. de Groot, wish to record their

indebtedness to S. F. C. H. Leyten for the assistance they received from him in this work.

The special version of the program, the second subject dealt with in this issue, has been developed by A. K. de Groot. To this end, he replaced the calculation of the stiffness matrix on the basis of an assumed displacement field by an approach based on finite-difference analysis. Thus the earlier experience gained in the investigation of columns has, though in modified form, been incorporated, as it were, in the generally applicable STANIL program. The new version developed in this way is known as STADIF. The two programs STANIL and STADIF can be used side by side, the actual choice between them being dependent on the nature of the problem and on the future users' preference. STANIL ties up more closely with general non-linear finite-element method programs, and STADIF offers greater accuracy in cases where plastic hinges occur.

Application of the non-linear program STANIL to the overall safety of frames with imperfect connections

1 Statement of the problem

CUR-VB Committee C28 "Structural details" tested a number of beam-to-column connections in order to obtain some idea of the strength of such connections in framed structures. Fig. 1.1 shows the test set-up and an experimentally determined load-deflection curve. If the connection were perfect and if the beam and column behaved in a linearly elastic manner, the diagram would comprise a straight ascending portion up to the point where plastic behaviour occurs. Then the diagram would become horizontal. These two portions of the diagram together characterize what is sometimes called the elasto-plastic behaviour of the beam-to-column connection.

In the analysis of framed structures it is generally assumed that elasto-plastic behaviour can indeed be taken into account. As Fig. 1.1 shows, however, the experimental results may be unsatisfactory in that the experimentally obtained strength values are liable to fall rather far short of the calculated ones. Since the connections which were tested has been analysed and designed fully in accordance with the Netherlands code of practice VB74, it may well be asked whether there may not be existing structures, or structures yet to be built, which, though conforming to the code, do not attain the desired level of safety. The test results indeed raise the question why then no problems have arisen in practice. The Committee accordingly studied the question as to what the practical consequences are of somewhat deficient strength and stiffness of the connection, with particular reference to the extent of the decrease in the expected overall safety of a framed structure. The present authors were associated with that research.

This part of the publication presented here reports on a study which was carried out with a view to obtaining information on the sensitivity of framed structures to imperfections in the connections. Such information is required also because of the considerable scatter displayed by the test results. The investigations comprised two parts. The first of these is concerned with braced frames (sidesway prevented), subjected to vertical loading only. The second part deals with unbraced frames (sidesway permitted), which are

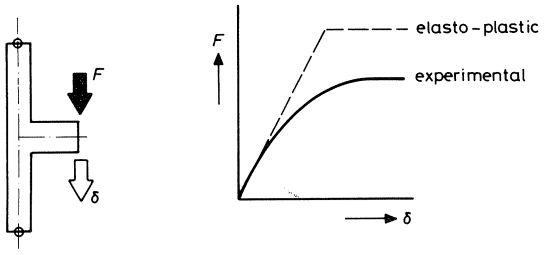

Fig. 1.1. Test set-up for beam-to-column connection.

subjected not only to vertical but also to horizontal loading, so that they present a more difficult problem.

Both these types of frame, i.e. braced and unbraced, are conceived as comprising several storeys. The stiffness ratios of the columns and beams are assumed to be so chosen that the columns have points of zero bending moment at mid-height within each storey. Investigation can then be confined to a portion comprised between two successive points of zero moment, as shown in Fig. 1.2. It is furthermore assumed that a single-bay and a two-bay frame will consitute the most unfavourable cases. Frames with more than two bays contain a larger number of internal nodes, for which the expectations are less pessimistic.

The procedure adopted in this research is as follows. The frame is designed with the aid of linear elastic theory. The bending moments are calculated on the assumption that the columns and beams are prismatic members and that the beam-to-column connections are completely rigid. The reinforcement is assumed to be adapted to the variation in bending moment found to occur in the members. Plastic moments which develop when the loading is increased are presumed theoretically all to occur simultaneously at a load factor $\gamma = 1.7$. Since the connection does not actually conform to the ideal conception, however, failure of the structure may occur at a lower value of the load factor. This lower value is determined on the basis of the actual behaviour of the part more particularly considered within the frame.

This behaviour could be derived from the behaviour of the column, the behaviour of the beam and the behaviour of the connection. These three behaviour components will presumably be non-linear. In the actual research conducted here, a somewhat different procedure was adopted, however. For the analysis of the column and of the connection the above-mentioned experimental results were used, and the behaviour of the beam was analysed with the STANIL program. The residual safety of a framed structure is determinable by combination of this experimental result and this computational result.

In order to explain the procedure, first a theoretical analysis of the problem will be presented, in which the beam is still conceived as an elastic member in which a plastic hinge suddenly achieves full development. Then follows a specific application with the aid of the STANIL program, which gives a more realistic description of the behaviour of the (cracked) beam.

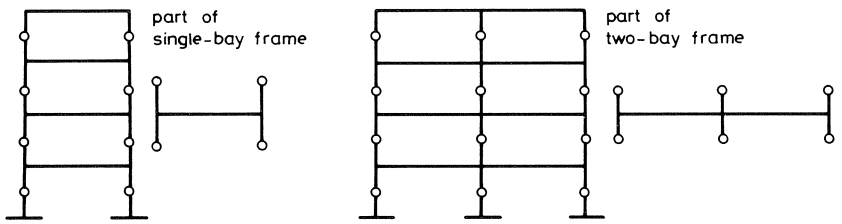

Fig. 1.2. A representative portion of a single-bay and of a two-bay framed structure is investigated.

2 Theoretical analysis of a braced single-bay frame

2.1 *Modeling the problem*

The frame envisaged in Fig. 2.1 is, as already stated, assumed to be reinforced in accordance with linear elastic theory. The four pin joints (hinges) cannot undergo horizontal displacement. Under working load conditions the uniformly distributed load q acts on the structure; the load factor γ then has the value 1.0. If γ is increased to 1.7, the full plastic moment will be attained both at mid-span of the beam and at the beam-to-column connections. Each column is of course provided with appropriate reinforcement. The load factor γ (or, stated somewhat differently, the overall structural safety) can, however, increase to the value 1.7 only if the connection is able to resist the full plastic moment of the beam.

We shall consider a load factor γ which is greater than 1.0 but smaller than 1.7 and shall investigate what happens if the connection is not perfect. The frame is shown again in Fig. 2.2; the zones in which the full plastic moments occur are represented by the hatched areas. The sections 1 and 2 divide the frame into three parts. The parts to the left of section 1 and the part to the right of section 2 each comprise the column and the connection. The part situated between these two sections will more particularly be referred to as the "beam". The state parameters at sections 1 and 2 will play an important part in the calculations. For reasons of symmetry the bending moment M and the rotation φ are equal at these two sections. This is indicated in Fig. 2.3.

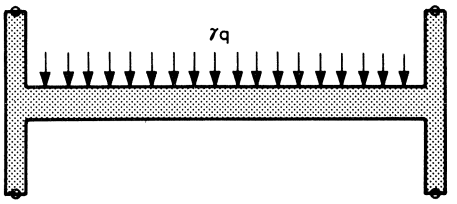

Fig. 2.1. Braced single-bay frame under vertical loding.

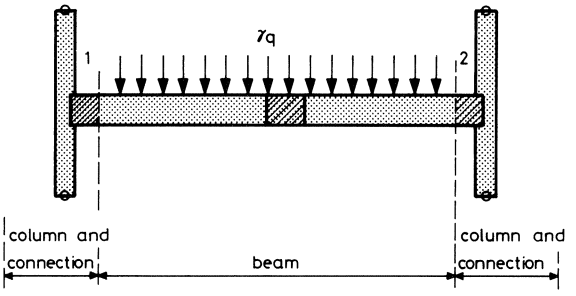

Fig. 2.2. What is meant by the designations "column and connection" and "beam".

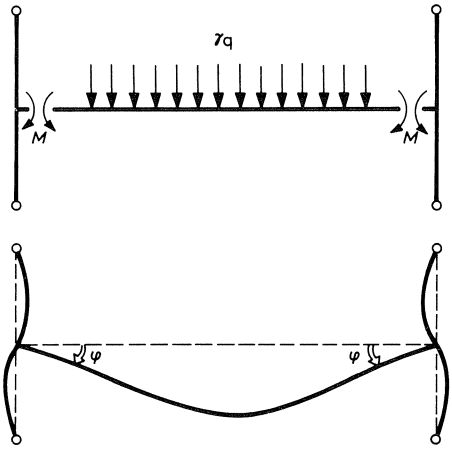

Fig. 2.3. The quantities M and φ at the section between the "column and connection" and the "beam" determine the analysis.

The structural part comprising "column and connection" will, in the case of an ideal connection, behave as shown in Fig. 2.4a, representing the highly stylized M-φ diagram; in reality the rigidity will be somewhat less when cracking occurs in the column. The strength of the connection is expressed by the factor γ_c, the capacity of the connection. For an ideal connection this factor will have the value $\gamma_c = 1.7$. In that case the full plastic moment associated with the vertical loading on the frame as a whole with $\gamma = 1.7$ will just be able to develop.

What is meant by an imperfect connection is shown in Fig. 2.4b. The structural part comprising "column and connection" is now less rigid, but also less strong. The value of γ is less than 1.7, which means that the vertical loading cannot be increased as much. Therefore the maximum γ that the structure can resist is likewise smaller than 1.7.

The analysis which will now be presented aims to determine the maximum value of the overall safety γ for a given capacity γ_c of the connection. This will be done in two steps. First, the frame is analysed for a chosen loading level γ and a chosen capacity γ_c of the connection. Then a method of determining the maximum γ that can be resisted is developed.

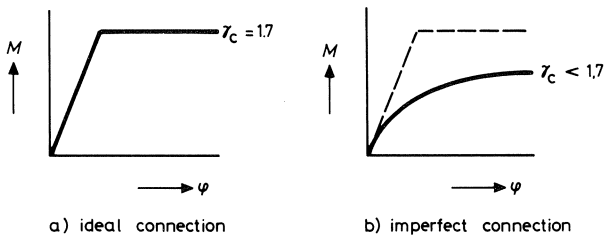

Fig. 2.4. Definition of an ideal and of an imperfect connection.

2.2 *Analysis of the frame for one chosen loading level γ and a chosen capacity γ_c of the connection*

An experimentally determined M-φ diagram is available for the "column and connection", and the M-φ diagram applicable to the beam is calculated with STANIL. The two diagrams are shown in Fig. 2.5; their point of intersection determines the values of M^* and φ^* which will occur in this frame for the chosen values of γ and γ_c.

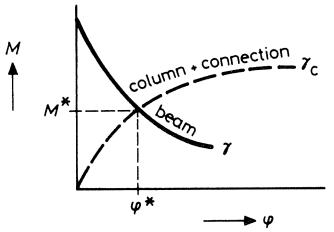

Fig. 2.5. Determination of M^* and φ^* for one chosen loading level γ and a given capacity γ_c of the connection.

M-φ diagram for the "column and connection"

The experimental results obtained for the "column and connection" mentioned in the introduction, are not directly available in the form of an M-φ diagram. The tests were performed as shown in Fig. 1.1., yielding an F-δ diagram as the result. In order to obtain from this the M-φ diagram for the "column and connection" it is necessary first to correct the F-δ diagram for the deflection of the short horizontal portion of the beam. With the aid of the STANIL program it was calculated what the F-δ diagram of this portion would be if the "column and connection" were infinitely rigid. On subtracting this from the overall F-δ diagram the F-δ diagram for the "column and connection" comprising an infinitely rigid beam portion is obtained. Then, by rescaling the axes from F to Fe and from δ to δ/e, the required M-φ diagram for the "column and connection" is obtained, see Fig. 2.6.

The rotation φ cannot become infinitely large. At a certain value - the rotational capacity - the connection will fail. The tests show this value to be $\varphi = 0.0103$ radians.

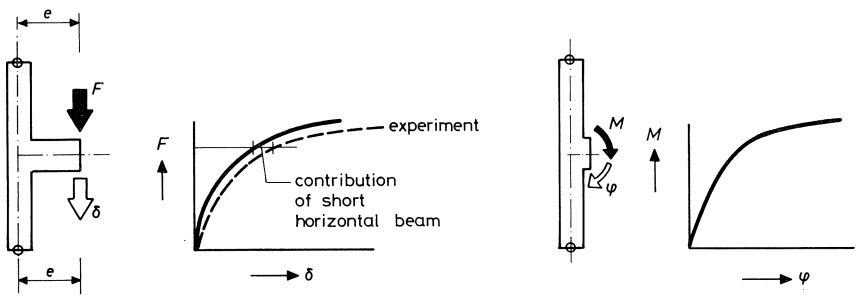

Fig. 2.6. Translation of the recorded F-δ relation into the required M-φ relation.

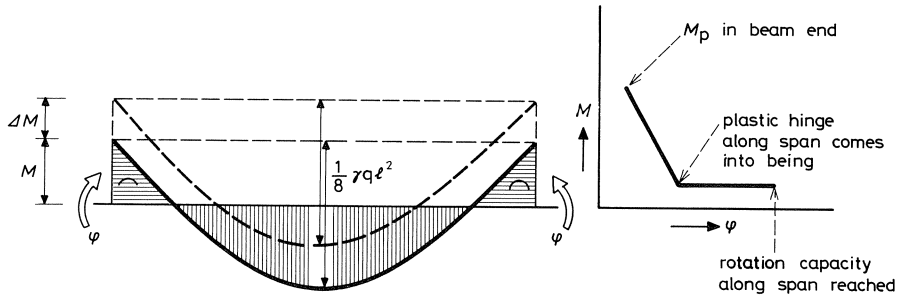

Fig. 2.7. Method of determining the M-φ diagram of the beam.

M-φ diagram for the beam

The M-φ diagram for the beam, for a particular chosen value of γ, can be determined entirely by calculation. In Fig. 2.7 the solid curve represents a possible bending moment diagram for the beam. The sagitta (or "rise") of the parabola is $\frac{1}{8}\gamma q l^2$. The bending moment M acts at the end of the beam. It can be calculated what angular rotation φ corresponds to this moment. The dash line in Fig. 2.7 represents a second bending moment diagram, which is valid for the same load q, but shifted vertically a distance ΔM. Now a different moment M acts at the end of the beam, and a different (smaller) rotation φ occurs. The value of ΔM can increase until the full plastic moment M_p at the end of the beam is just attained. By so choosing ΔM that M decreases we cause the mid-span moment to increase and therefore φ likewise to increase. If the beam behaves elastically, φ increases linearly and M decreases linearly until the full plastic moment in the span is attained. A plastic hinge then develops in the span of the beam. The bending moment diagram cannot undergo further displacement (M remains constant), but the rotation φ can still increase. A mechanism is formed until the rotational capacity at the plastic hinge is exceeded. This situation corresponds to a horizontal branch in the M-φ diagram. In reality the beam does not behave in such an elastic/ideally plastic manner as assumed here. In consequence of cracking and gradual extension of the plastic zone the M-φ diagram for the beam will be curved, as already shown in Fig. 2.5. The actual shape of the diagram can be calculated with the aid of the STANIL computer program.

2.3 *Determination of the maximum resistable loading level γ for a given capacity γ_c of the connection*

From the foregoing it is now known how the M-φ curve for the beam can be determined for a chosen value of the loading level γ. We can perform this calculation for a number of values of γ, so that a whole family of M-φ curves for the beam is obtained. By intersecting this family with the M-φ curve for the "column and connection" it can be determined what extreme value of γ is possible. Fig. 2.8 illustrates this procedure for $\gamma_c = 1.1$.

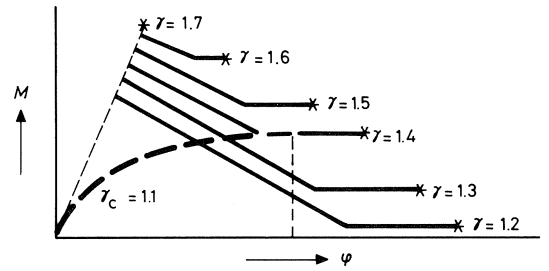

Fig. 2.8. Determination of the largest γ for a chosen $\gamma_c = 1.1$.

In the example presented here the M-φ curve for the "column and connection" will intersect the M-φ curves for the beam so long as γ is smaller than, or equal to, 1.4. The overall structural safety would, in this example, therefore have decreased from 1.7 to 1.4 if the safety of the connection were to undergo the considerable decline from 1.7 to 1.1. Part of Fig. 2.8 has been reproduced in Fig. 2.9, which shows how, for the maximum value of γ, the values of M and φ have changed in relation to the expected values associated with an ideal connection ($\gamma_c = 1.7$).

2.4 *Sensitivity analysis*

With one further step we obtain direct insight into the effect of γ_c upon γ. For this purpose we intersect all the M-φ curves of the beam with all conceivable M-φ curves for a connection. This is shown schematically in Fig. 2.10. It can at once be seen what maximum value γ corresponds to a given γ_c. From this information a curve such as that plotted in Fig. 2.11 can then be obtained quite simply. If this diagram represents the behaviour of a braced frame, there still remains a residual safety ($\gamma > 1.0$) for the overall structure, even if the capacity of the connection is very poor ($\gamma_c < 1.0$). In Chapter 3 the calculation will be performed for a specific case, which will confirm the validity of the approach embodied in the theoretical analysis presented here.

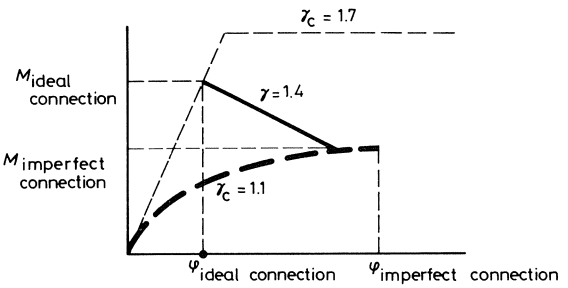

Fig. 2.9. At an imperfect connection the angular rotation increases considerably.

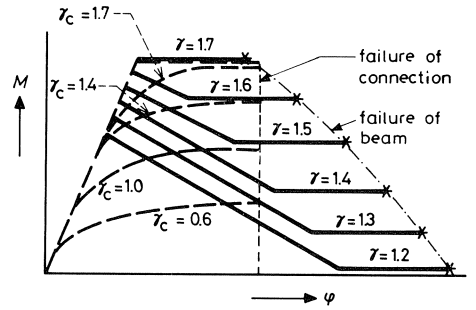

Fig. 2.10. Overall representation of all M-φ curves.

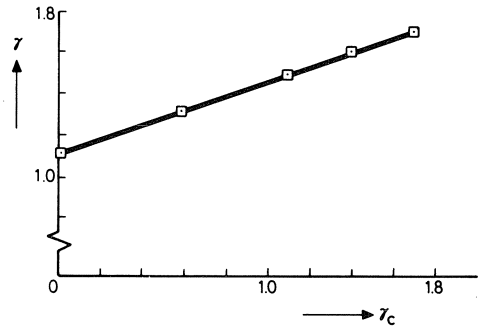

Fig. 2.11. Effect of the capacity γ_c of the connection upon the overall safety γ of a braced frame.

3 Application to a braced single-bay frame

3.1 *Structure*

The structure to be analysed is shown in Fig. 3.1. Its dimensions correspond to those of an actual framed structure as commonly encountered in practice, scaled down in a 1 : 2 ratio. It is to be designed in accordance with linear elastic theory, on the assumption of completely rigid connections. The bending moment diagram for the beam is then as shown in Fig. 3.2. The fixed-end reinforcement is taken as 1.04% of the full cross-section (1.11% of the effective cross-section), while the span reinforcement is taken as 0.96% of the full cross-section of the beam. In terms of elastic behaviour the span moment and the fixed-end moment then simultaneously attain the yield moment at a load $q_u = 59.2$ kN/m. The working load is $q = 59.2/1.7 = 34.8$ kN/m, which therefore corresponds to a load factor $\gamma = 1.0$.

The material properties to be introduced into the STANIL analysis are described with reference to the σ-ε diagrams in Fig. 3.3.

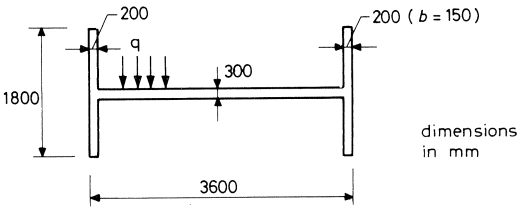

Fig. 3.1. Dimensions of a single-bay H-frame.

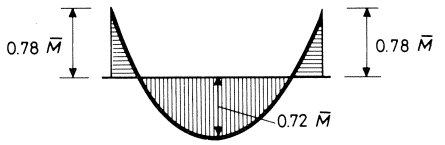

Fig. 3.2. Bending moment diagram for the beam, assuming elastic behaviour ($\bar{M} = \frac{1}{12}ql^2$).

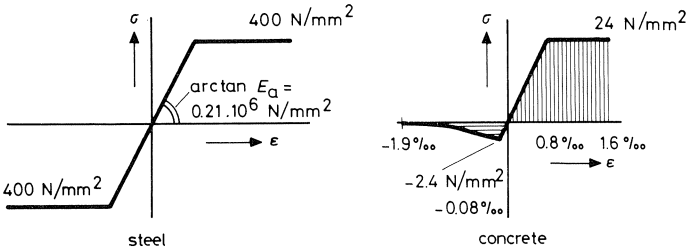

Fig. 3.3. Stress-strain (σ-ε) diagrams for concrete and steel.

3.2 *Results*

The M-φ curves calculated for the beam with STANIL are shown as solid lines in Fig. 3.4, while the dash lines in the same diagram represent a number of M-φ curves for the "column and connection", as might be obtained experimentally, after substraction of the behaviour of the beam calculated with STANIL, as already noted with reference to Fig. 2.6. For $\gamma_c = 1.7$ the diagram shows two curves, one based on elasto-plastic analysis and the other which holds experimentally. The highest value attained by the diagrams for $\gamma_c = 1.7$ is $M = 49.9$ kNm, since the connection has been designed for $q = 34.8$ kN/m or $q_u = 1.7 \times 34.8 = 59.2$ kN/m, while according to Fig. 3.2 a support moment occurs with magnitude $M = 0.78\ \bar{M} = 0.78 \times \frac{1}{12}ql^2 = 49.9$ kNm. The other γ_c curves terminate at

$$M = \gamma_c \times \frac{49.9}{1.7}$$

From Fig. 3.4 it appears that the rotational capacity of the beam in the case under inves-

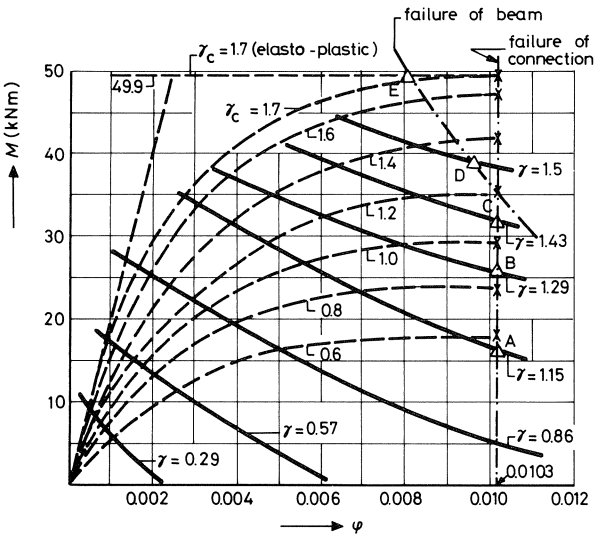

Fig. 3.4. M-φ curves for beam (——) and for column and connection (----) for a two-bay frame.

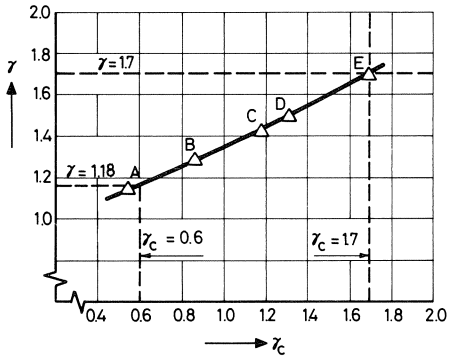

Fig. 3.5. Relation between γ and γ_c for single-bay frame.

tigation is often sufficiently large and that failure is mostly due to insufficient rotational capacity of the connection. Only for values of $\gamma > 1.45$, or for $\gamma_c > 1.2$, does the beam become the governing criterion. In Fig. 3.5 a number of failure points are indicated by small triangles. With reference to this diagram it can be noted that a decrease in the value of γ_c from 1.7 to 0.6 results only in a decrease from 1.7 to 1.18 in the value of γ.

If it had been presupposed that the rotational capacity was not of governing significance, elementary limit analysis could have been applied. On the assumption that the plastic moments at the ends of the beam and at mid-span are in the same proportion to each other as the reinforcement percentages, the value of γ associated with $\gamma_c = 0.6$ can be calculated as follows:

$$\gamma = \frac{\frac{0.6}{1.7} * 1.04 + 0.96}{1.04 + 0.96} * 1.7 = 1.13$$

This result is, within 5%, of the same magnitude as that of the (accurate) analysis performed. It can be stated that in fact the elementary collapse solution is valid. This is confirmed by Fig. 3.4, from which it is apparent that the capacity of the connection is practically always fully utilized. The reason why the (accurate) analysis yields a value for γ which is about 5% higher is that the STANIL program somewhat over-estimates the full plastic moment in the beam.

3.3 *Conclusion for braced single-bay frame*

If the safety of the connection decreases from $\gamma_c = 1.7$ to $\gamma_c = 0.6$, the safety of the braced structure decreases only from $\gamma = 1.7$ to $\gamma = 1.18$.

If the safety of the connection exceeds $\gamma_c = 1.2$, the beam constitutes the governing criterion. For values γ_c smaller than 1.2 the rotational capacity of the connection governs overall structural failure.

4 Theoretical analysis of a braced two-bay frame

The structure will again be divided into separate parts, as shown in Fig. 4.1, including the plastic zones. For reasons of symmetry only one bay is represented here. To the left of section 1 there is, as in the previous case, a structural part comprising a "column and connection", for which experimentally determined M-φ curves are available. Between section 1 and the axis of symmetry of the frame is the "beam". A fully plastic hinge can develop at two sections in this beam, namely, in the span and at the centre column (axis of symmetry). Now, with the two quantities M and φ at section 1, it is possible to control the analysis. The model shown in Fig. 4.2 will be used for the purpose. As in the case of

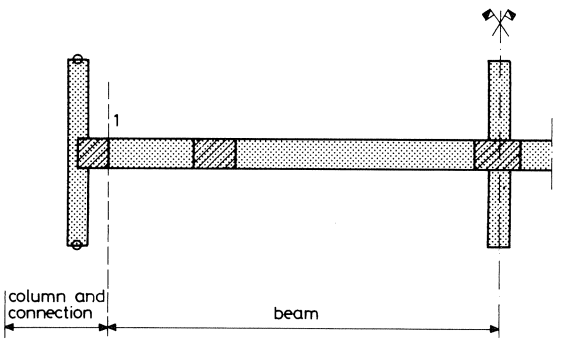

Fig. 4.1. Definition of "column and connection" and "beam" in a two-bay frame. Plastic hinges may form in the hatched regions.

the single-bay frame, the M-φ curve of the "column and connection" is intersected with the M-φ curve of the beam. The M-φ curve for the "column and connection" is the same as has already been discussed; that for the beam is somewhat different, but is determined in principle by a similar procedure to that described previously. This is shown in Fig. 4.3. If M decreases, φ will increase, and so will be bending moment at the axis of symmetry. When the latter moment becomes the plastic moment, an end hinge is formed. The beam then becomes less stiff. The rotation can still increase until the rotational capacity of the hinge has been exhausted. It is also conceivable that a second hinge develops in the span of the beam. The actual curves calculated with the STANIL program will be curved because of gradually developing formation of cracks and plastification.

The analysis procedure is similar to that for the single-bay frame. The family of M-φ curves of the "column and connection" and the family of M-φ curves of the "beam" are again plotted in the same diagram. In this way the effect of the safety γ_c of the connection upon the overall safety γ can be determined also for the two-bay frame.

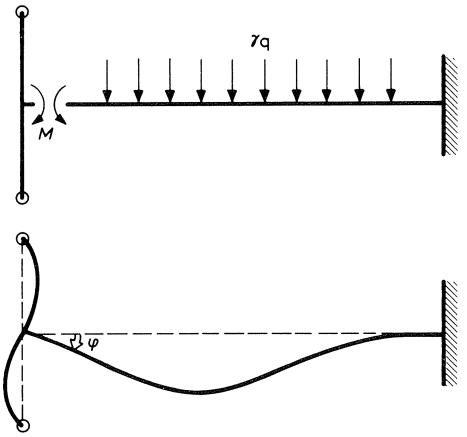

Fig. 4.2. The quantities M and φ at the section between "column and connections" and "beam" determine the analysis.

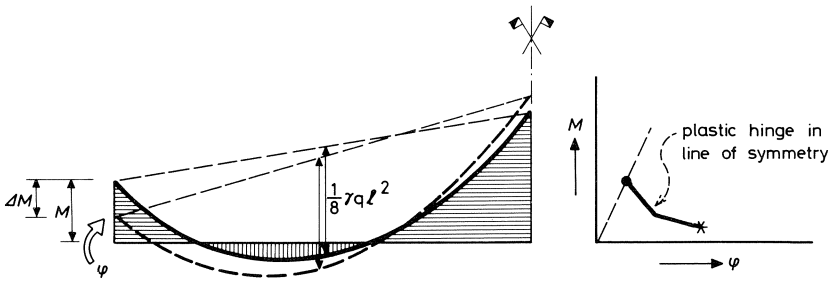

Fig. 4.3. Determining the M-φ curve for the beam.

5 Application to a braced two-bay frame

5.1 *Structure*

The structure to be analysed is shown in Fig. 5.1. The two-bay H-frame considered here is similar in respect of its geometry to the single-bay H-frame in Fig. 3.1. On the assumption of a completely rigid beam-to-column connection and on the basis of linear elastic theory we obtain the bending moment diagram represented in Fig. 5.2, which, for reasons of symmetry, need be considered only for one bay. The structure is designed for a working load $q = 35.2$ kN/m. The failure load is $q_u = 1.7 \times 35.2 = 60$ kN/m. The reinforcement is accordingly as follows:

left: 0.86%
centre: 0.86% of total cross-sectional area
right: 1.60%

The material properties are assumed to be as indicated in Fig. 3.3.

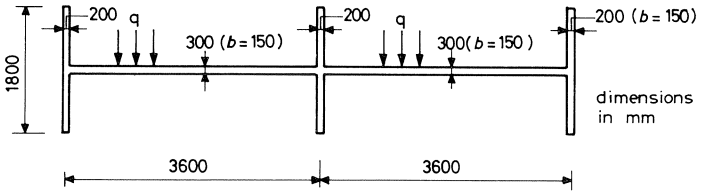

Fig. 5.1. Dimensions of two-bay H-frame.

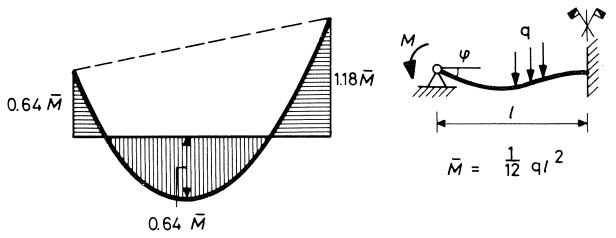

Fig. 5.2. Bending moment diagram for the beam, assuming elastic behaviour.

5.2 *Results*

The relation between M and φ of the left-hand support of the beam was again calculated with the aid of STANIL for a number of values of γ. The results are represented by solid lines in Fig. 5.3, while the dash lines in this diagram are again the M-φ curves for the "column and connection" as might be obtained from tests. According to Fig. 5.2 the maximum value for $\gamma_c = 1.7$ is:

$$0.64\bar{M} = 0.64 \times \frac{1}{12} q_u l^2 = \frac{0.64}{12} \times 60 \times 3.6^2 = 41.5 \text{ kNm}$$

For any value of γ_c the capacity of the connection is therefore:

$$M = \gamma_c \times \frac{41.5}{1.7}$$

There is found to be a characteristic difference between the results for a single-bay frame (Fig. 3.4) and those for a two-bay frame (Fig. 5.3). Because of the high percentage of reinforcement at the centre column the beam now has much less deformation capacity. This being so, the rotational capacity of the connection is indeed nowhere the governing criterion. In Fig. 5.3 the small triangles denote the points where failure of the beam occurs. The corresponding combination of γ and γ_c is indicated in Fig. 5.4. It appears that, despite the fact that $\gamma_c = 1.7$, the overall safety of the structure is no higher than 1.55, which is due to the elastic design approach adopted in which no account is taken of the shape of the M-φ curve of the connection. Against this, for values of γ_c lower than 1.7 the values of γ undergo only a small decrease. Thus, for $\gamma_c = 0.7$ it is found that γ is still relatively high at 1.3.

From Fig. 5.3 it can readily be seen when the (accurate) solution that has been obtained will agree most closely to the result of elementary limit analysis. The capacity of the connection is not fully utilized for any value of γ_c. However, the demand made upon this capacity increases according as γ_c is smaller, i.e., the elementary limit analysis offers a more closely valid approximation as γ_c decreases.

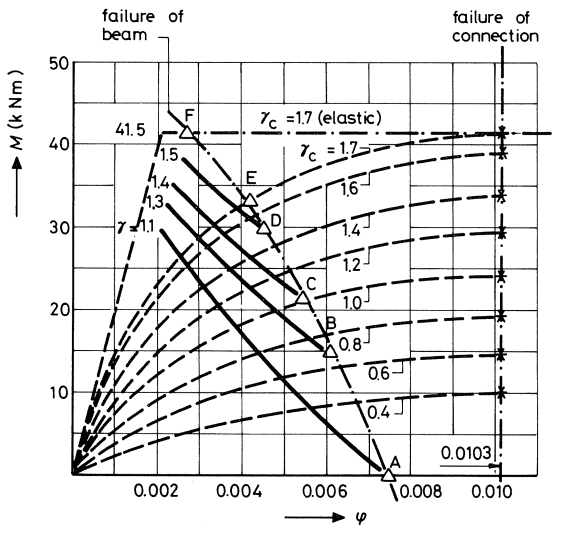

Fig. 5.3. M-φ curves for beam (——) and for column and connection (----) for a two-bay frame.

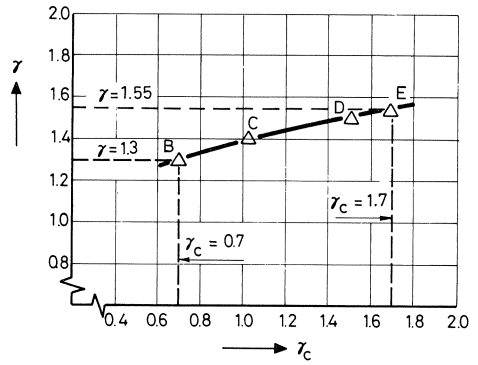

Fig. 5.4. Relation between γ and γ_c for two-bay frame.

5.3 *Conclusion for braced two-bay frame*

If the safety of the connection is $\gamma_c = 1.7$, the overall safety of the structure turns out to be lower, namely, $\gamma = 1.55$. If γ_c decreases from 1.7 to 0.7, the corresponding decrease in overall safety is merely from $\gamma = 1.55$ to $\gamma = 1.3$. The structure fails in the beam, the rotational capacity of the connection being greater than that of the beam.

6 Theoretical analysis of an unbraced single-bay frame

6.1 *Modeling the problem*

Fig. 6.1 shows a representative portion of a framed structure which is subjected not only to a vertical uniformly distributed load q, but also a transverse force (shear) S due to wind and second-order effects due to sidesway. The frame under consideration is again assumed to have been designed on the basis of linear elastic theory. The reinforcement determined in this way is, on account of the reversibility of the transverse force, arranged symmetrically in the structure. Under working load conditions the loads S and q are acting. If the load is increased 1.7-fold ($\gamma_S = 1.7$ and $\gamma_q = 1.7$), a collapse mechanism develops because a fully plastic hinge is formed at the right-hand beam-to-column connection and, simultaneously, in the span of the beam. This planned state of failure is denoted by the hatched plastic zones in Fig. 6.2.

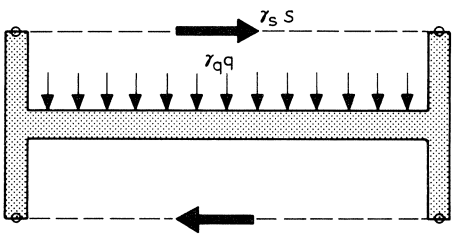

Fig. 6.1. Unbraced single-bay frame under vertical and horizontal loading.

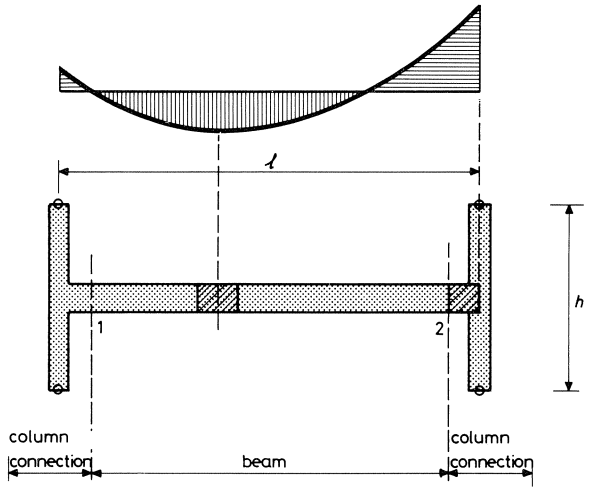

Fig. 6.2. Definition of "column and connection" and "beam".

In order to determine how this frame behaves if the connection is imperfect, two sections 1 and 2 are again applied. The behaviour of the beam between these sections will be determined analytically. In this part of the beam a full plastic moment can occur only in the span. To the left of section 1 and to the right of section 2 a "column and connection" will be considered, for which experimentally determined results are available.

The quantities M_1 and φ_1 at section 1 are not equal to the quantities M_2 and φ_2 at section 2 and will therefore have to be considered separately for these respective sections. Their positive sign convention is shown in Fig. 6.3.

6.2 *Analysis of the frame for chosen loading levels γ_S and γ_q and a given capacity γ_c of the connection*

"Column and connection" behaviour

The left-hand "column and connection" is subject to a deformation which is now not φ_1, but θ minus φ_1. The angle θ determines the sidesway, more particularly the tilt, of the frame. This tilt is equal on the left and on the right, so that the two "column and connection" parts undergo different deformations if φ_1 is not equal to φ_2. The experimentally determined M-φ diagrams should now be read as M_1-$(\theta$-$\varphi_1)$ and M_2-$(\theta$-$\varphi_2)$ diagrams respectively, as shown in Fig. 6.4.

"Beam" behaviour

The behaviour of the beam cannot now be described with an M-φ diagram. There is an M_1-φ_1 diagram for the end at section 1 and an M_2-φ_2 diagram for the end at section 2. These diagrams are moreover interlinked and can be established for a particular (fixed) choice of γ_S and γ_q, as appears from Fig. 6.5. For a chosen value of γ_S the total bending moment to be resisted due to the horizontal shear forces has the value $\gamma_S Sh$. This must be equal to M_2 minus M_1, so that the difference of the two moments is constant.

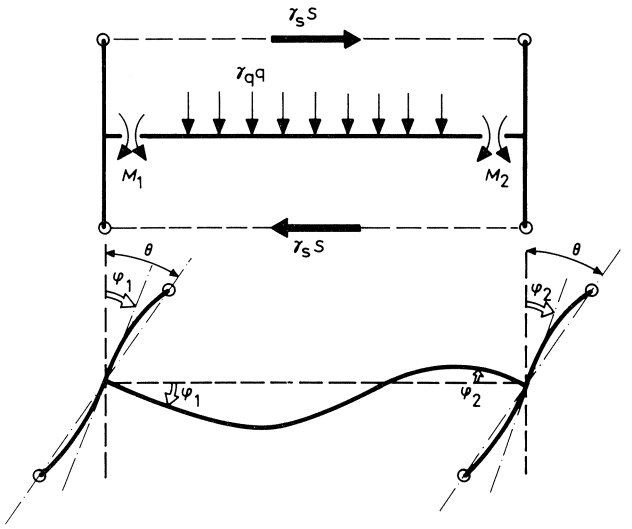

Fig. 6.3. The quantities M_1, φ_1, M_2 and φ_2 at the sections, also the angle of tilt θ.

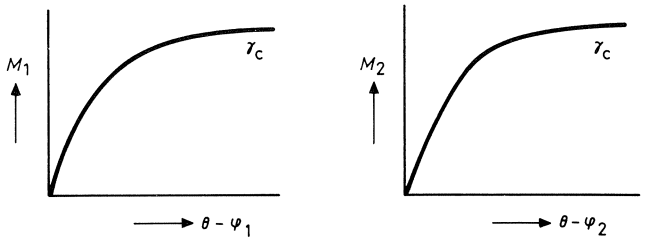

Fig. 6.4. Moment-deformation diagrams for the "column and connection".

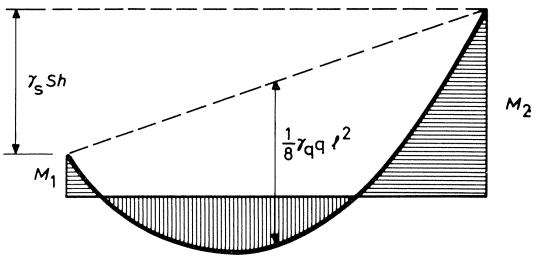

Fig. 6.5. Initial assumption for beam behaviour.

In the same way as has been done in the case where only vertical loading acts on the structure, the bending moment diagram in Fig. 6.5 can as a whole be shifted upwards or downwards parallel to its original position. Thus, different sets of (interlinked) values of M_1 and M_2 are obtained, and also different values of φ_1 and φ_2 for each shifted position of the diagram. If the beam behaves in a purely elastic manner, φ_1 and φ_2 will, when the parallel shift is applied, increase by equal amounts, but of opposite sign. In a φ_1-φ_2 diagram the pairs of values thus move along a line at 45°, as indicated in Fig. 6.6. This line terminates at one end when the full plastic moment just develops at section 2, and at its other end this line changes into a line sloping at a different angle when a plastic hinge develops in the span of the beam (formation of a mechanism). This line continues until the rotational capacity in the span has been exhausted.

We now have at our disposal four components for the final calculation, namely, two M-φ diagram for the "column and connection" parts in Fig. 6.4 and two M-φ diagram for the "beam" in Fig. 6.6. We must intersect these in pairs in order to determine the values M_1^*, φ_1^*, M_2^* and φ_2^* which fit in with the chosen loading level and the given safety of the connection. The angle of tilt θ must moreover be calculated. The problem can be worked out quite simply by drawing all four diagrams in one composite graph, as has been done in Fig. 6.7. On the lines relating to the two ends of the beam 1 and 2 the points corresponding to each other have been marked by the same letter (a to f). The two lines for the "column and connection" parts to the left of 1 and to the right of 2, respectively, coincide to form a single line and have here been plotted in the reverse position in rela-

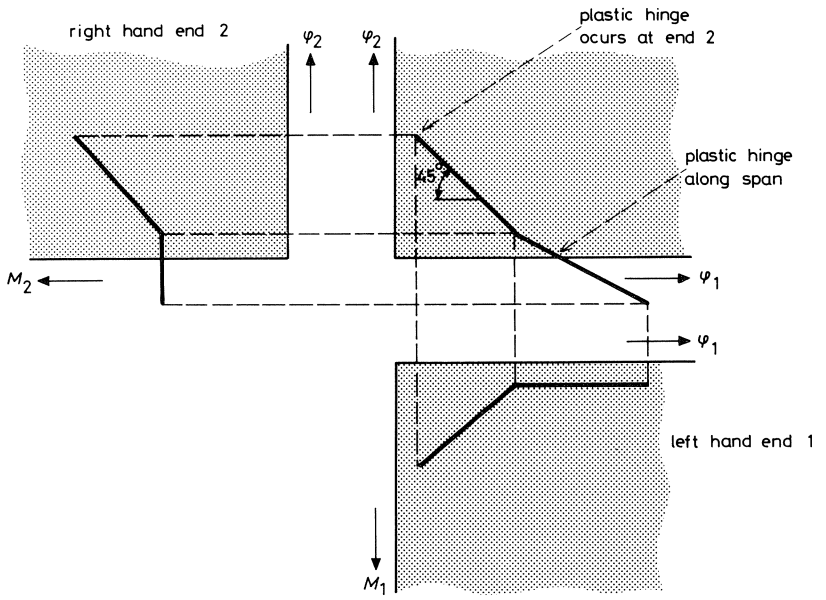

Fig. 6.6. The M_1-φ_1 and M_2-φ_2 diagrams for the ends of the beam are interlinked through the φ_1-φ_2 diagram.

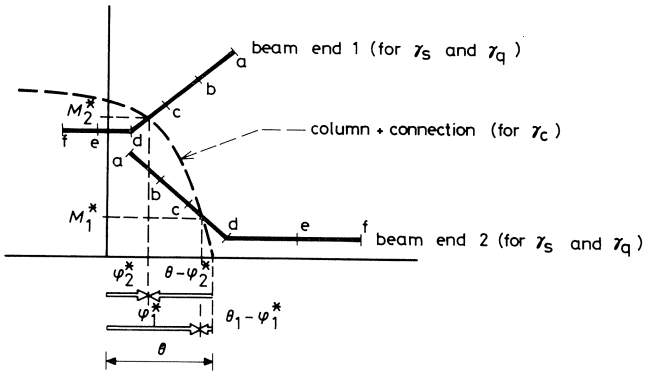

Fig. 6.7. Determination of M_1^*, φ_1^*, M_2^* and φ_2^* for a chosen loading level γ_S and γ_q and a given capacity γ_c of the connection.

tion to Fig. 6.4. This line is so shifted horizontally that the line for beam end 1 and the line for beam end 2 are intersected at points corresponding to each other. In the example presented in Fig. 6.7 this occurs between the points marked c and d. The angle of tilt θ can now be directly read as the horizontal distance between the origin of the M-φ diagrams of the beam end and the origin of the M-φ diagram of the "column and connection" parts. The ends of the beam have then passed through the deformations φ_1^* and φ_2^*, and the "column and connection" parts through the deformations $\theta - \varphi_1^*$ and $\theta - \varphi_2^*$, respectively.

6.3 *Determination of the maximum resistable loading level γ_S for a chosen loading level γ_q and a given capacity γ_c of the connection*

If it is desired to know the loading that can be resisted for a given capacity of the connection, there are several alternative loading procedures that can be applied. The first possibility is to increase γ_S and γ_q equally. A second method consists in keeping γ_q constant and increasing only γ_S. The first of these alternatives is a pessimistic assumption because in actual practice more particularly the vertical loading will not increase much. Partly because the present investigation aims to explain why no mishaps have occurred in practice, the second alternative will now be worked out, γ_q being kept constant and given the value 1.0 (in reality even this working load assumption will very seldom occur). For a given capacity γ_c of the connection we can then determine the maximum γ_S that can still just be resisted. The analysis explained in **6.2** must, for this purpose, be repeated for a number of values of γ_S. In this way two families of M-φ curves are obtained, for the beam ends 1 and 2, respectively. These families must be intersected with the curves of the "column and connection" parts, which will move farther and farther to the right because the tilt θ increases with increasing γ_S. The procedure is similar in principle to that applied to braced frames in Fig. 2.8, but is only somewhat more laborious. Fig. 6.8 shows an example where $\gamma_q = 1.0$ and $\gamma_c = 1.4$ has been chosen.

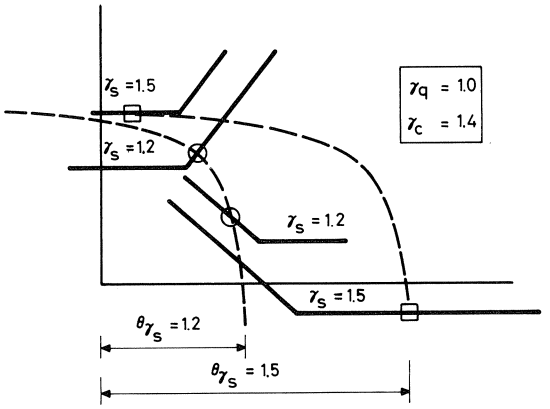

Fig. 6.8. Determination of maximum γ_S for chosen γ_q and given γ_c.

Two curves of each of the two families have been drawn. Two values for γ_S have been introduced. For $\gamma_S = 1.2$ the strength of the connection is not fully utilized; but for $\gamma_S = 1.5$ the ultimate strength is utilized, so that this is the highest value of γ_S that is still possible for this capacity $\gamma_c = 1.4$ of the connection.

6.4 *Sensitivity analysis*

Finally, the sensitivity of the overall unbraced framed structure to imperfections of the connections will be summarized here. As has been done for braced frames in Fig. 2.11, in the present case, too, the maximum γ_S can be plotted against the value of γ_c. In order to draw this diagram the calculation set forth in **6.3** must be repeated for various values of the capacity γ_c of the connection. The result will be as shown in Fig. 6.9. In comparison with the corresponding diagram in Fig. 2.11 for braced frames an unbraced frame is more sensitive to a decrease in γ_c. It should be borne in mind, however, that for a perfect connection ($\gamma_c = 1.7$) the value of γ_S can become much higher, since the vertical loading has been put at $\gamma_q = 1.0$, while the structure has in fact been designed for the loading levels $\gamma_S = 1.7$ and $\gamma_q = 1.7$.

6.5 *Second-order effect*

So far, no attention has been paid to the second-order effect. With the results obtained it is, however, possible to gain some insight into this. The schematic representation in Fig. 6.1 for unbraced frames must, for this purpose, be supplemented with a vertical normal force N acting in the structure (Fig. 6.10). When sidesway occurs, this force will produce an additional horizontal shear θN. The total shear S_N is therefore composed of a contribution $\gamma_S S$ due to wind and a contribution θN due to the second-order effect:

$$S_N = \gamma_S S + \theta N \tag{1}$$

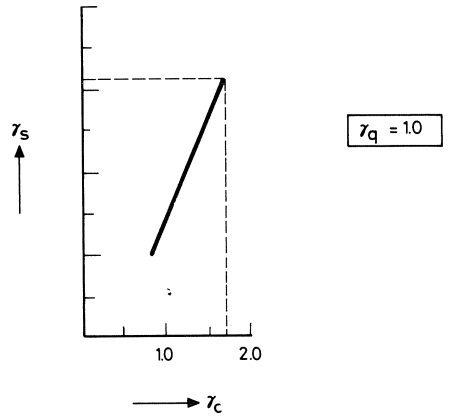

Fig. 6.9. Effect of the capacity γ_c of the connection on the overall safety γ_S of an unbraced frame.

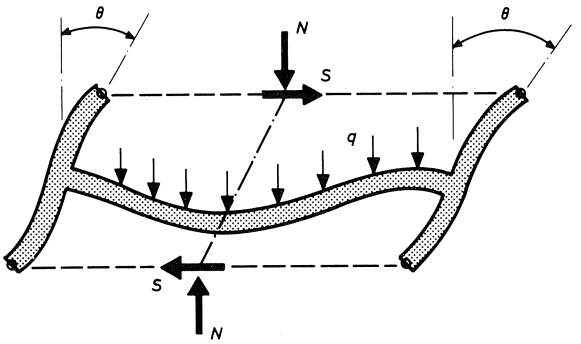

Fig. 6.10. Second-order effects give rise to an extra horizontal shear θN.

For S_N we may write $\gamma_{SN} S$. Actually, Fig. 6.9 represents the relation between γ_{SN} and γ_c. In order to obtain from this the relation between γ_S and γ_c we can write for (1):

$$\gamma_{SN} S = \gamma_S S + \theta N$$

whence we obtain:

$$\gamma_S = \gamma_{SN} - \frac{\theta N}{S} \tag{2}$$

The magnitude of N will depend approximately on the number of storeys (n) in the framed structure. Then the following approximation will hold for the bottom storey:

$$N = n \cdot ql$$

so that (2) becomes:

$$\gamma_S = \gamma_{SN} - n\theta \frac{ql}{S} \tag{3}$$

We have thus obtained a formula for correcting the results, as shown in Fig. 6.9, for the second-order effect. The factor ql/S is a constant in the formula. The tilt θ can be read from the diagrams for any value of γ_{SN}. In principle, the adjusted diagram will be as shown in Fig. 6.11. According as n increases the value of γ_S decreases.

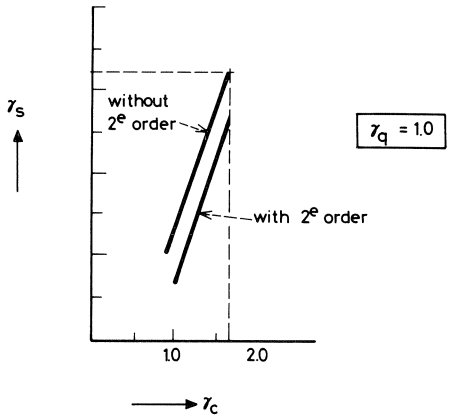

Fig. 6.11. Effect of the capacity γ_c of the connection on the overall safety γ_S of an unbraced frame, with and without second-order effect.

7 Application to an unbraced single-bay frame

7.1 *Structure*

The frame to be analysed is shown in Fig. 3.1 and also in Fig. 7.1. Besides a uniformly distributed load $q = 34.82$ kN/m there is a transverse force (shear) $S = 16.34$ kN acting on the structure, which is designed for $\gamma_q = \gamma_S = 1.7$, i.e., for $q_u = 1.7 \times 34.82 = 59.2$ kN/m and $S_u = 1.7 \times 16.34 = 27.8$ kN. The bending moment diagram, for elastic behaviour, is given for $\gamma_q = \gamma_S = 1.0$ in Fig. 7.2. The support reinforcement is determined for section 2, where $M_u = 74.8$ kNm, requiring a steel percentage of 1.65%, while the span reinforcement for $M_u = 46.2$ is 1.05% (percentages referred to gross cross-section). In the STANIL analysis both the span reinforcement and the support reinforcement are assumed to be present over the whole length of the beam. As in the two preceding worked examples, the σ-ε diagrams given in Fig. 3.3 have been adopted. The M-φ relations for the connections will have to be shifted about, as explained with reference to Fig. 6.8, in order to find the highest possible value of γ_S. Accordingly, the M-φ relations for the connections are presented separately in Fig. 7.3. This diagram includes these relations also for negative values of φ, since (as will appear in due course) the support

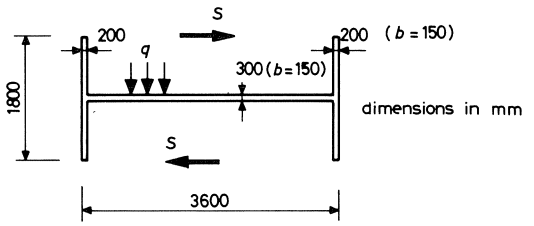

Fig. 7.1. Dimensions of single-bay H-frame mat in mm = dimensions in mm.

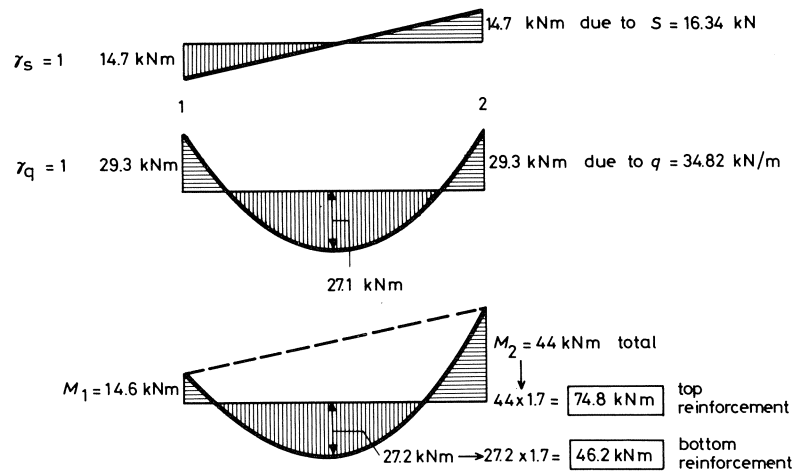

Fig. 7.2. Bending moment diagram of beam, assuming elastic behaviour.

moment at M_1 is liable to change its sign. The M-φ curve designated by $\gamma_c = 1.7$ does of course again attain the failure moment (in this case $M_u = 74.8$). For the other values of γ_c the maxima are situated at $74.8 \times \gamma_c/1.7$. The diagram based on elastic behaviour is likewise indicated for γ_c, while the rotational capacity of the connection again corresponds to the limit 0.0103.

7.2 *Results*

Figs. 7.4 and 7.5 show M_1-φ_1 and M_2-φ_2 curves calculated with STANIL for two values of γ_S, namely, $\gamma_S = 1.0$ (low) and $\gamma_S = 3.0$ (high). For the vertical load q the value $\gamma_q = 1.0$ is adopted. These diagrams also include some M-φ curves (shown as dash lines) from Fig. 7.3. These curves have been shifted in the manner described in **6.3**. The value of γ_c for which the structure fails can be accurately determined by interpolation. For a low value of the shear ($\gamma_S = 1.0$) a low capacity of the connection ($\gamma_c = 0.81$) will suffice, and the moments in the beam are of limited magnitude (see Fig. 7.4). In the case of a high value of the shear ($\gamma_S = 3.0$) the situation changes (see Fig. 7.5): a high capacity of the connection is then required, and much larger moments occur at the end of the beam.

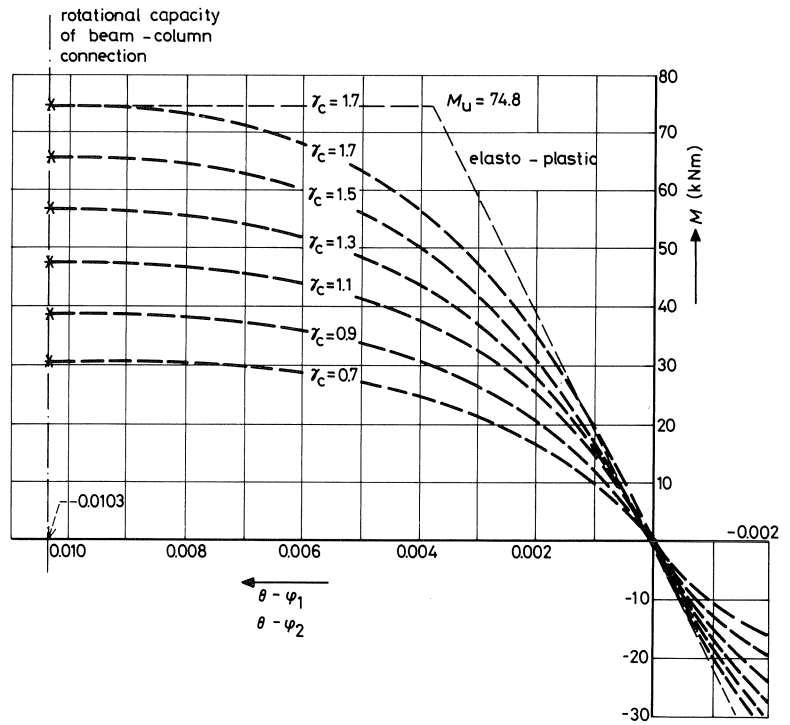

Fig. 7.3. M-φ relation for beam-to-column connection rotational capacity of beam-to-column connection elasto-plastic.

In all cases failure is caused by the rotational capacity of the beam-to-column connection being exceeded. Only if intersection points were to occur on the horizontal branch of the M_1-φ_1 and M_2-φ_2 curves, respectively, could the rotational capacity of the beam be the determining criterion. With the large shear ($\gamma_S = 3.0$) the plastic hinge in the span develops; but there is then as yet no question of the rotational capacity being exhausted. Besides γ_c, the associated tilt θ (sidesway) is also indicated in Figs. 7.4 and 7.5. The values obtained for γ are assembled in Fig. 7.6 and plotted as a function of γ_S in the manner presented in Fig. 6.11. In order to determine the result taking in due account the second-order effect, it is necessary to know the number of storeys in the structure. The magnitude of the shear for which this frame has been designed corresponds to approximately four storeys. This is the assumption adopted in Fig. 7.6 for the purpose of the design calculation.

It is to be noted that in this diagram the upper part of the relation between γ_S and γ_c is shown as a dash line and that an upper limiting value of $\gamma_S = 2.84$ has been imposed. The reason for this is as follows. So far, it has been assumed that the top reinforcement is present over the whole length of the beam. In reality, however, the top reinforcement will extend to the point of zero bending moment. The most unfavourable combination of loads for which this zero moment point has to be determined in the design is represent-

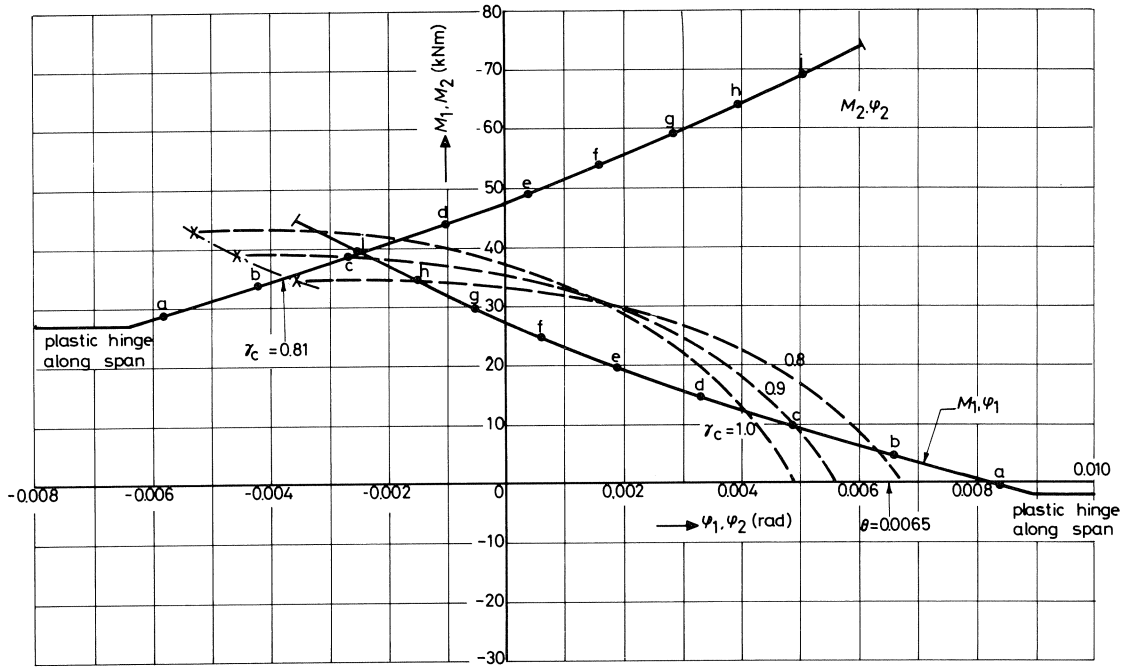

Fig. 7.4. Determination of required γ_c in order to obtain $\gamma_S = 1$ for $\gamma_q = 1$.

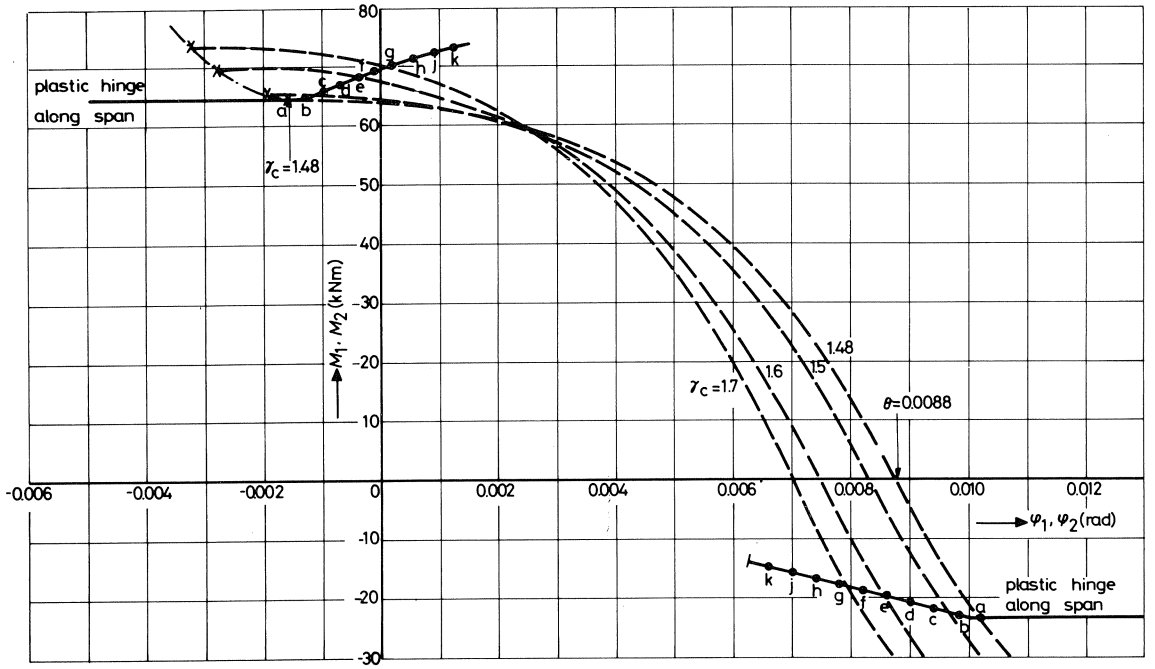

Fig. 7.5. Determination of required γ_c in order to obtain $\gamma_S = 3$ for $\gamma_q = 1$.

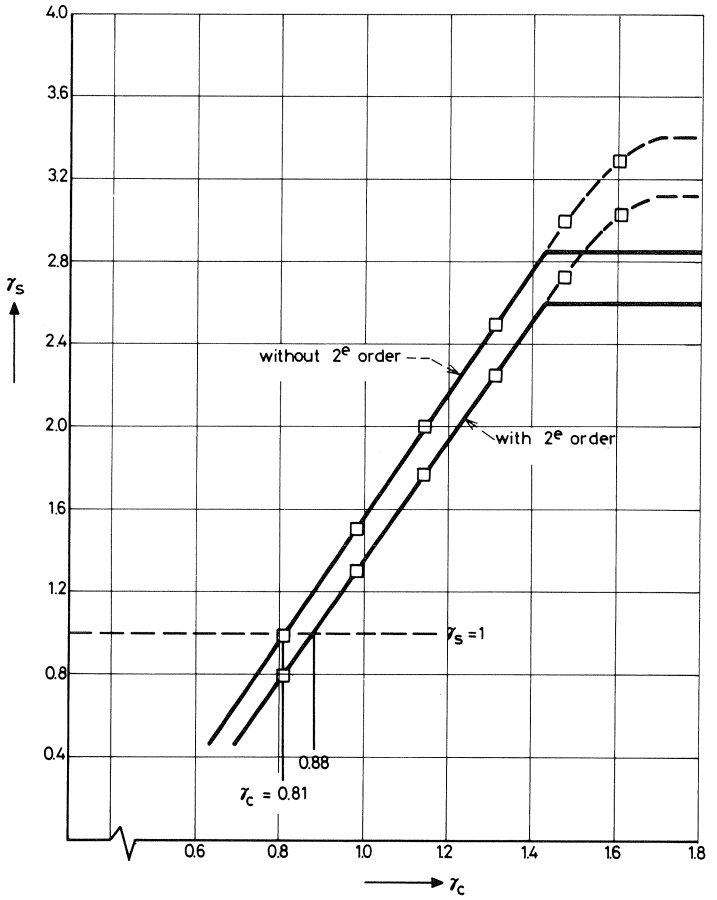

Fig. 7.6. Effect of the capacity γ_c of the connection on the overall safety γ_S of an unbraced frame with $\gamma_q = 1$.

ed by $\gamma_q = 1.0$ and $\gamma_S = 1.7$, from which, on the basis of an elastic analysis, a length of 900 mm is found. The STANIL calculations showed, however, that in the region represented by the dash lines in Fig. 7.6 the negative support moment extended beyond the above-mentioned 900 mm, with the result that the structure would fail prematurely.

It turns out that the load factor γ_S can in fact increase far above the value 1.7. This is because the structure has been designed for loading in which both the shear and the vertical load are increased by a factor of 1.7. In the research envisaged in this report the factor adopted for the vertical load is 1.0, in which case the factor for the horizontal load can be expected to go above 1.7. If the capacity γ_c of the connection becomes low, the load factor γ_S nevertheless decreases to below 1.7. The capacity γ_c must, however, become manifestly less than 1.0 before the situation is reached where even the horizontal working load can no longer be resisted.

A closer inspection of Figs. 7.4 and 7.5 leads to the following conclusion. For a high value of γ_c (associated with Fig. 7.5) a full plastic moment develops both at the connec-

tion and in the span of the beam. In that case the solution provided by elementary limit analysis is therefore valid. For a low value of γ_c (Fig. 7.4) a fully plastic hinge does not develop in the span because the rotational capacity of the connection is not sufficiently high for that to occur. The structural safety is then less than would follow from elementary collapse analysis. For $\gamma_c = 0.8$ the elementary analysis would indicate $\gamma_S = 1.55$, whereas in reality a value of no more than $\gamma_S = 0.96$ is found, as is seen from Fig. 7.6.

7.3 *Conclusions for an unbraced frame*

In order to obtain overall structural safety greater than corresponding to $\gamma_S = 1$ the value of γ_c must be not less than 0.88. This is apparent from Fig. 7.6, from which the influence due to the second-order effect is immediately ascertainable. Exceeding the rotational capacity of the beam-to-column connection is always the cause of failure.

8 Conclusions

The investigation reported here was carried out with a view to finding out what consequences an imperfect beam-to-column connection has upon the overall safety of a structure. In order to provide a general answer, the results of the analysis are summarized for the range $0.7 < \gamma_c < 1.7$ in Fig. 8.1.

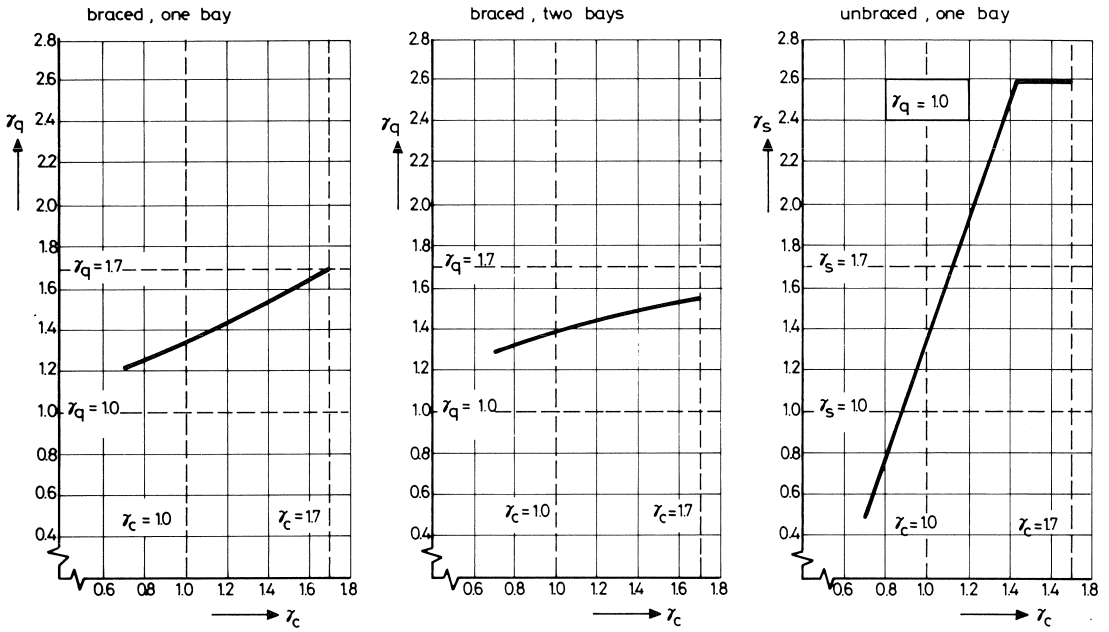

Fig. 8.1. Summary of all combinations of highest possible load factors and connection capacities.

In the braced frames investigated the maximum possible load factor (or in other words: the overall safety of the structure) does indeed decrease, but remains above the value 1.0. This would still be the case even if the connection were so poor as not to be able to resist even the working load ($\gamma_c < 1$). There is found to be little difference between single-bay and two-bay frames. However great the variation in the strength of the beam-to-column connection, it still always remains possible to resist the working load.

The unbraced frame investigated is found to be more sensitive to variation in the strength of the beam-to-column connection. In the range for γ_c under consideration the safety of such a frame decreases from 2.6 to 0.5, whereas the corresponding decrease for a braced frame is merely from 1.7 to 1.2. Yet this does not cause difficulties in practice, since the working load ($\gamma_S = 1.0$) can be resisted so long as the capacity of the connection is not less than $\gamma_c = 0.9$. In unbraced frames, too, considerable variation in the strength of the beam-to-column connections can occur without this having any noticeable effects on existing buildings.

It was also investigated whether it would have been permissible to apply elementary limit load analysis. For the single-bay braced frame this is indeed do. However, for the two-bay braced frame such analysis is permissible only for small values of γ_c. For large values of γ_c there is not sufficient rotational capacity in the beam span. In the case of an unbraced single-bay frame the elementary limit analysis may be used only for large values of γ_c. If the value of γ_c is low, the rotational capacity of the beam-to-column connection is seriously deficient, so that the safety falls short of what elementary limit analysis suggests.

Notation

b	width of beam or column
e	eccentricity of load in experiment
F	load in experiment
l	span of beam
M	bending moment acting on beam-to-column connection
ΔM	increment of M
$\bar{M}$	reference value of bending moment ($\frac{1}{12}ql^2$)
M_1	bending moment at left-hand end of beam
M_2	bending moment at right-hand end of beam
M^*	final moment at beam-to-column connection
M_p	ultimate (plastic) bending moment
N	normal force in the frame
n	number of storeys
q	vertical distributed load on beam
q_u	ultimate value of q
S	total horizontal shear force in frame
S_u	ultimate value of S
δ	displacement in experiment

σ stress
ε strain
γ load factor (safety)
γ_S load factor (safety)
γ_{SN} local quantity
γ_q load factor (safety)
γ_c capacity of the connection (safety)
φ rotation of beam-to-column connection
φ_1 rotation of left-hand end of beam
φ_2 rotation of right-hand end of beam
φ^* final value of rotation
θ angle indicating the tilt of the frame (due to sidesway)

Development of STADIF, a special version of the program, on the basis of finite differences

9 Introduction

It has already been stated in the Preface that the new program called STADIF for the non-linear analysis of reinforced concrete plane framed structures is a modification of the STANIL program, as elaborated by Gouwens [4] in 1974. In that program an assumed displacement field is considered in which the displacements perpendicular to the axis of the member conform to a third-degree curve, while those in the direction of the axis are described by a second-degree curve chosen for the purpose. The essential feature of STADIF is that it does not use an assumed displacement field, but that always the actual displacement field is calculated by the application of finite-difference analysis for each member. The great advantage of this procedure is that along the entire axis of the member equilibrium between the external and the internal forces is obtained. In the method with the assumed displacement field this equilibrium exists only between the external and the internal nodal forces, which often gives rise to difficulties in correctly interpreting the results of the calculations. This is explained in Fig. 9.1. The member shown in Fig. 9.1a, made of reinforced concrete with the cross-section shown in Fig. 9.1b and σ-ε diagrams as presented in Fig. 9.1c, undergoes deformation in consequence of loading which acts at the ends.

In an analysis with STANIL a state of equilibrium is attained as shown in Fig. 9.1d. The solid line indicates the so-called internal bending moment curve which is obtained

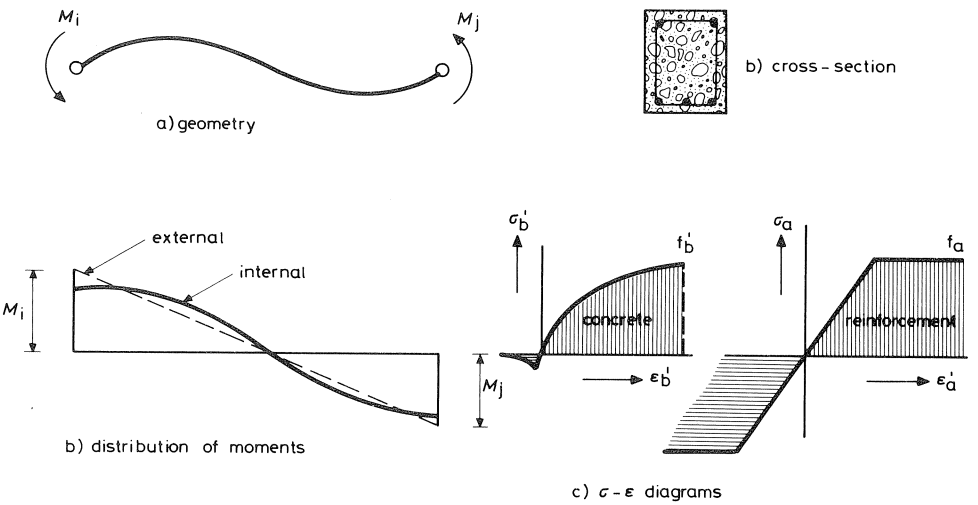

Fig. 9.1. In the method with the assumed displacement field no equilibrium exists between the external and internal forces along the axis of the member.